JOURNAL OF THERMOPHYSICS AND HEAT TRANSFER
Vol. 21, No. 2, April–June 2007

Ion Injection as an Effective Technique of Heat Transfer Enhancement in Space

Daniele Testi*
University of Pisa, 56126 Pisa, Italy

DOI: 10.2514/1.24977

The heat transfer enhancement technique of ion injection is studied in point-plane geometry. A downward-facing plate is uniformly heated in a pool, filled by the dielectric liquid HFE-7100. The application of a high voltage between the high-curvature electrode and the plate induces a strong jetlike motion, impinging on the heat transfer surface, for which the temperature field is mapped by thermochromic liquid crystals. Heat transfer coefficients are enhanced up to 1800%, with a negligible power input. At heat-flux values typically generated by electronic components, the heat exchange phenomenon is almost entirely controlled by the electrical forces acting within the fluid, whereas buoyancy plays only a minor role, making the technique very attractive for use in a free-falling object.

Nomenclature

A	=	plate wetted area, m^2
c	=	fluid specific heat, $J \cdot kg^{-1} \cdot K^{-1}$
d	=	point-to-plate distance, m
er	=	relative error
g	=	acceleration due to gravity, $m \cdot s^{-2}$
HV	=	applied voltage, V
L	=	plate characteristic thermal length, m
Nu	=	local Nusselt number
$\langle Nu \rangle$	=	mean Nusselt number on the plate
p	=	plate wetted perimeter, m
q	=	heat flux, $W \cdot m^{-2}$
R	=	radius of curvature of the point electrode's tip, m
Ra	=	local Rayleigh number
$\langle Ra \rangle$	=	mean Rayleigh number on the plate
T	=	temperature, K
x	=	location along the shorter side of the plate, with respect to the midpoint, m
y	=	location along the longer side of the plate, with respect to the midpoint, m
α	=	convective heat transfer coefficient, $W \cdot m^{-2} \cdot K^{-1}$
β	=	fluid coefficient of cubic expansion, K^{-1}
λ	=	fluid thermal conductivity, $W \cdot m^{-1} \cdot K^{-1}$
Λ	=	insulator thermal conductivity, $W \cdot m^{-1} \cdot K^{-1}$
ν	=	kinematic viscosity, $m^2 \cdot s^{-1}$
ρ	=	fluid mass density, $kg \cdot m^{-3}$

Subscripts

b	=	bulk
f	=	film
max	=	maximum
w	=	wall

I. Introduction

THE present work is part of a broader research activity, mainly funded by the Italian Space Agency (ASI) and the European Space Agency (ESA), investigating the effect of the electrical and the gravitational force fields under various heat transfer regimes. Reference [1] gives a comprehensive review of these studies, aimed at gaining a better understanding of the basic phenomena and enhancing the heat exchange performances both on ground and in space. Particularly, in single-phase convection, heat transfer can be greatly enhanced by applying direct-current electric fields to dielectric liquids.

Because of the high complexity of fluid dynamics under electric fields, researchers have mainly followed an approach of empirical observation of the involved phenomena. References [2,3] review the valuable experimental work carried out, respectively, in the U.S. and Japan. Although high heat transfer rates have been obtained in a variety of different configurations, the process has turned out to be critically influenced by the geometry (shape, radius of curvature, presence of microasperities, and orientation), the composition, and the polarity of the high-voltage electrode, as well as by the chemical, thermophysical, and electrical properties of the working fluid.

The present work deals with an unexplored regime: a downward-facing heated plate impinged by an ionic jet, leaving from a point electrode. In addition, a novel liquid, HFE-7100, has been chosen for its electrochemical stability, necessary for the long-term performance of the electrohydrodynamic (EHD) technique.

Different heat-flux values are applied to assess whether buoyancy has a role in the heat exchange phenomenon or whether the present configuration is completely dominated by the electrical forces.

II. Theoretical Background

Ion injection from a high-voltage metallic point (the emitter) in an electrically insulating liquid has already proved to be a very efficient technique for cooling down a surface, greatly enhancing convective heat transfer coefficients, with a negligible power input [4–7].

A sufficiently high dc electric field (on the order of 10^6–10^7 $V \cdot m^{-1}$) in the proximity of a sharp electrode produces, through complex electrochemical reactions [8], ions of the same polarity as the emitter. As a consequence, the created free charge, entraining the adjacent neutral molecules, induces a motion directed toward the facing grounded electrode [9] and is capable of augmenting the transfer coefficients on its surface. In terms of thermofluid-dynamic behavior, an analogy can be drawn between submerged impinging jets and the EHD-induced flow [7].

The injection strength is controlled by the high-field electrochemistry of the metal/liquid interface [10]. Therefore, at a given high voltage, the process is critically influenced by the chemical nature of the dielectric fluid and by the curvature, the composition, and the polarity of the emitting electrode.

Received 5 May 2006; revision received 23 November 2006; accepted for publication 29 November 2006.

*Ph.D. in Energetics, Researcher, Department of Energetics "L. Poggi," via Diotisalvi 2.

In a nonpolar, insulating liquid, electrochemical properties are determined by the extrinsic molecules having high electrodonor or electroacceptor qualities. These impurities have a strong influence on the rate of ion formation. Also, the rate easily changes over a wide range by changing the concentration of an impurity [11]. On the contrary, polar molecules can dissolve a great variety of species and are more likely to take part directly in the chemical reactions. In this way, they turn out to be almost insensitive to the concentration of any particular impurity, and the emission of ions is more likely to go on at stable rates. As a drawback, polar molecules require larger power consumption, owing to their higher electrical conductivity. In fact, for a small increase of permittivity over the value of 2, the resistivity can drop off many orders of magnitude [8], and Joule heating losses within the dielectric may become relevant at high voltages.

In the experimental campaign described in [12], performances of different emitters have been compared. These tests have shown that a stainless steel point under negative polarity, in combination with HFE-7100 as the operating fluid, gives particularly high and stable heat transfer rates.

III. Experimental Apparatus

To evaluate the performance of the ion injection mechanism in terms of heat transfer enhancement, a proper experimental apparatus has been built, allowing a high-voltage point electrode to be easily mounted perpendicularly to a grounded, heated plate at an adjustable distance.

A. Fluid

The working fluid chosen for the present experimental campaign is the weakly polar dielectric HFE-7100, a hydrofluoroether produced by 3M^{TM}. The main physical properties of the liquid are reported in Table 1. HFE-7100 consists of two inseparable isomers with essentially identical properties (see Fig. 1).

HFE-7100 is nonflammable, nontoxic, and colorless. It is thermally and chemically stable, compatible with a wide range of metals, plastics, and elastomers, and has no ozone depletion potential, together with other favorable environmental characteristics. In addition, it complies with the strict safety specifications needed for flying in space, even on manned vehicles. All these notable properties, together with its low freezing point and its particularly low viscosity, make HFE-7100 appropriate for applications such as heat sinks for space.

Its electrical resistivity is high enough to guarantee negligible Joule dissipation, even when the intensity of the electric field in the vicinity of the sharp electrode is almost as high as the fluid dielectric strength.

B. Test Specimen

The liquid fills a transparent polycarbonate resin (Lexan®) vessel, for which the main elements are shown in Fig. 2.

The inner dimensions of the pool are 130 (height) $\times$ 200$\times$ 170 mm. The stainless steel plate is 113 $\times$ 109 mm, with a 5-mm thickness. It is uniformly heated by an electrical resistance heater attached above it. A 60-mm-thick layer of thermal insulator [$\Lambda = 0.038\ \mathrm{W \cdot m^{-1} \cdot K^{-1}}$] covers the upper face of the vessel. Type-T thermocouples are mounted at different locations within the insulator for detecting heat losses, which have been negligible for the entire campaign.

Table 1 HFE-7100 physical properties (T is expressed in °C)

Chemical name	Methoxy-nonafluorobutane
Chemical formula	$C_4F_9OCH_3$
Electrical resistivity, $\Omega \cdot m^{-1}$	3.29×10^7
Dielectric strength	1.10×10^7
Relative permittivity	7.39
Boiling point, °C	61 (at 1 bar)
Freezing point, °C	−135
Density, $kg \cdot m^{-3}$	$1538.3 - 2.269 \times T$
Kinematic viscosity, $m^2 \cdot s^{-1}$	$4.958 \times 10^{-7} - 5.952 \times 10^{-9} \times T + 3.571 \times 10^{-11} \times T^2$
Specific heat, $J \cdot kg^{-1} \cdot K^{-1}$	$1133 + 2.00 \times T$
Thermal conductivity, $W \cdot m^{-1} \cdot K^{-1}$	$0.0737 - 0.000195 \times T$
Coefficient of expansion, K^{-1}	$2.269/(1538.3 - 2.269 \times T)$

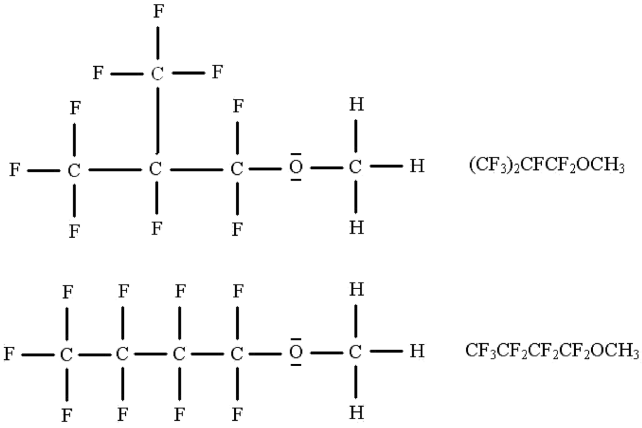

Fig. 1 Chemical structure of the isomers of HFE-7100.

The brass rod supporting the point is inserted in a PTFE (Teflon®) screw, which can move along its axis, fixing the distance between the high-voltage electrode and the grounded plate.

Depending on the orientation of the test pool, the heated plate can be upward-facing, downward-facing, or vertical. In the present campaign, to minimize the effect of buoyancy forces, it is placed downward-facing.

A thin, transparent plastic plate, located at a 25-mm distance from the metallic plate, divides the pool into a lower and an upper region, preventing significant mass transfer between the two areas. Water coming from a thermostatic bath flows inside the copper tube in the lower region, which functions as a heat sink. In this area, the liquid is stirred by a fan to reduce the thermal resistance between the plastic dividing wall and the cooling water. Instead, the EHD-induced flow is confined to the upper part of the pool, for which the bulk temperature is measured by two more type-T thermocouples. All the thermocouples are connected to a zero-point reference junction and have an accuracy of ± 0.2 K.

An expansion vessel with an elastic rubber cap on top is used to keep the fluid at ambient pressure and compensate the volume increase that the liquid undergoes during the heating process.

A dc reversible-polarity high-voltage power supply is capable of imposing up to 30 kV on the brass rod and, consequently, on the emitter. A picoammeter measures the current passing through the fluid, on the order of 10^{-6} A, with a relative accuracy of 0.4%. The instrument is protected against an incidental electrical discharge, as illustrated in Fig. 3.

The high-voltage electrode is just a regular tailor's pin made of steel. From an image taken under the microscope, the radius of curvature of its tip (see Fig. 4) can be estimated at about 0.1 mm.

C. Thermographic Technique

The optical method of liquid crystal thermography is employed for monitoring the temperature on the heated plate. In particular, a 0.15-mm sheet of encapsulated thermochromic liquid crystals (TLCs) in the cholesteric phase is directly stuck to the bottom wetted side of the metallic plate. The sheet (manufactured by Liquid Crystal Devices, Inc.) consists of a polyester film (Mylar®), with a substrate of black paint, over which a 10-μm liquid crystal layer is deposited.

Two 650-W halogen lamps of 20-cm diameter illuminate the plate with a white light. The lamps are positioned on the opposite sides of the vessel and produce a quasi-cylindrical light beam. A Nikon E995 digital camera is placed on a tripod in front of the vessel, focusing on the liquid crystal sheet, which is viewed under an angle of about 40 deg (see Fig. 5).

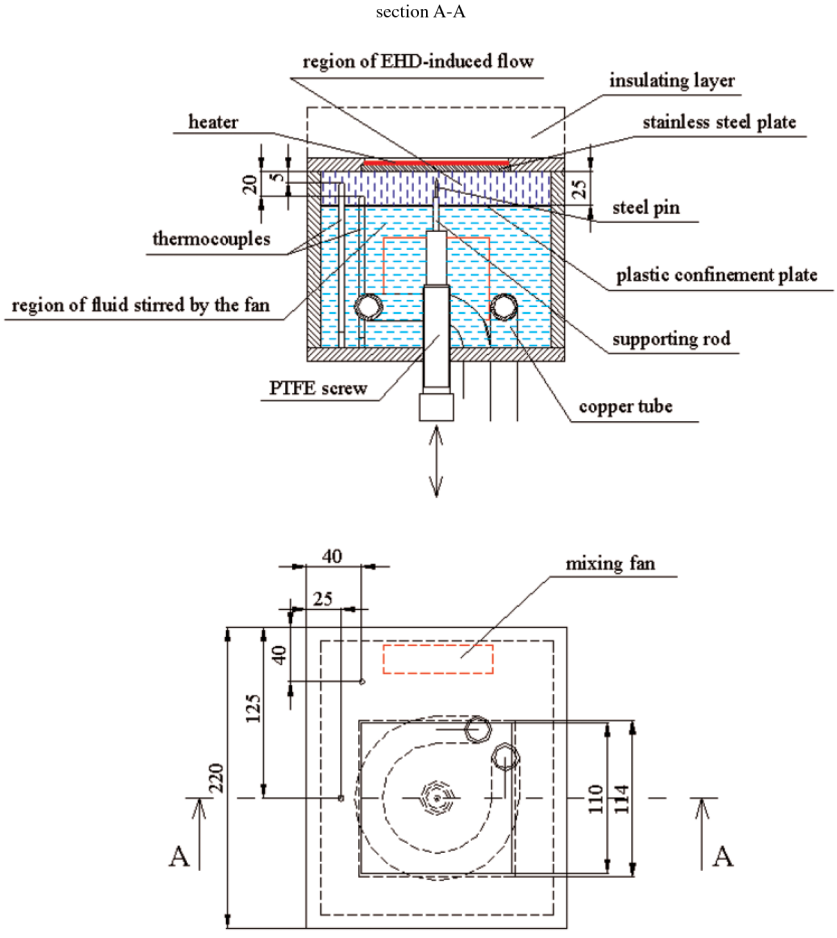

Fig. 2 Drawing of the test specimen.

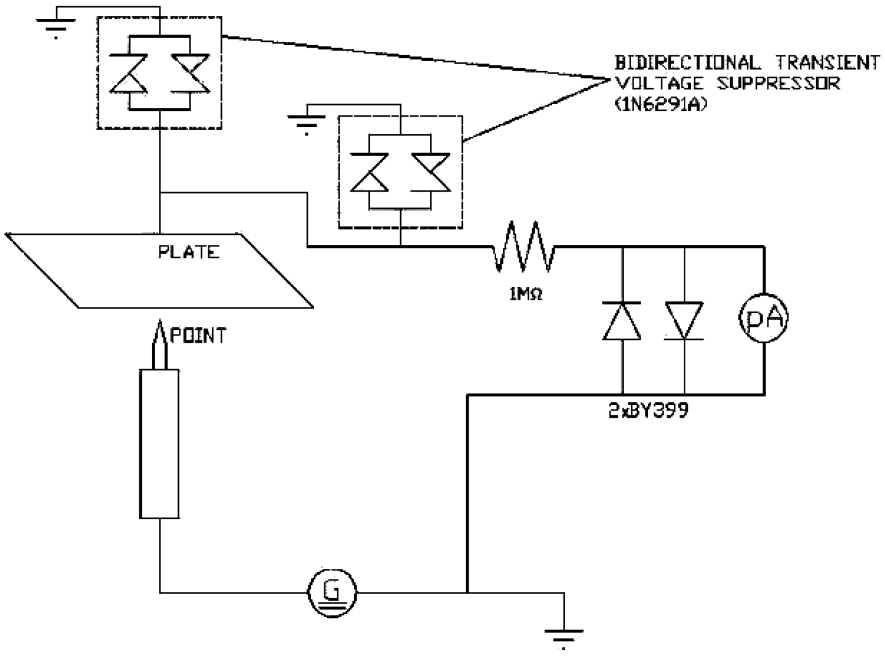

Fig. 3 Scheme of the high-voltage electrical circuit.

Most of the submerged elements are painted black to avoid reflections. However, shadows cast by the submerged thermocouples and by the central support cannot be entirely eliminated. In addition, the central rod covers a small part of the heat transfer surface from view.

The employed TLCs have a color-play interval of 2 K, going from 29.1 to 31.1°C. The relationship between chromaticity and temperature for each point of the sheet has been found by a nontrivial calibration procedure, described in detail in [13], giving an overall accuracy of ±0.1 K.

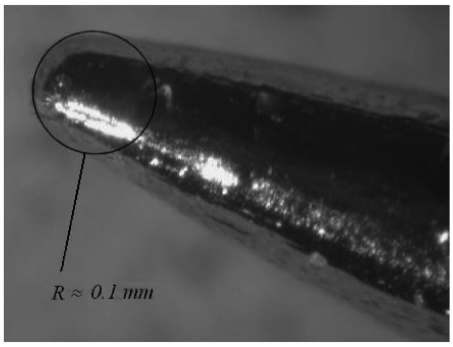

Fig. 4 Image of the pin, taken under the microscope.

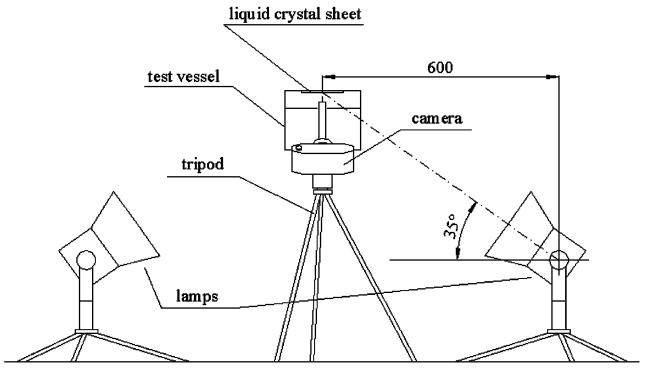

a)

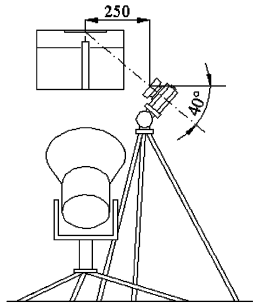

b)

Fig. 5 Relative position of the vessel and of the liquid crystal sheet with respect to the tripod and the lamps: a) front view and b) lateral view.

IV. Test Procedure and Data Analysis

After distillation and degassing of the liquid, the pin has been "aged" under a negative 30 kV voltage for over 100 h, to eliminate nonuniformities on the emitting surface.

Subsequent to these preliminary operations, three sets of tests have been conducted at different heat-flux values: $q = 690$, 1380, and 3080 $\mathrm{W \cdot m^{-2}}$. Each set is formed by three tests at the following voltage values: $HV = -30$, -27, and -21 kV. The point-to-plane distance has been fixed at $d = 20$ mm, because a previous experimental campaign [14] has shown that the heat transfer characteristics of the phenomenon under exam are almost insensitive to d in the range from 8 to 20 mm.

In every test, a steady-state condition is awaited (taking care to regulate the temperature in the thermostatic bath) to obtain wall temperatures within the color-play interval of the TLCs. At the higher heat fluxes, this has not been possible on the entire heat transfer surface; thus, a reduced area has been mapped, excluding the zones on the sides of the plate.

A photograph of the liquid crystal sheet is manually taken with the digital camera, rapidly switching the lamps on and off to avoid a significant radiative heating on the plate. Afterwards, the recorded image is processed by a computer, to evaluate, when possible, the temperature pattern.

The thermocouples' signals are acquired by the scanner of a digital multimeter and transferred to a computer, together with the current sent by the picoammeter. The data gathered by the computer are recorded on files and processed in real time by Labview™, using Matlab® scripts as the interface for mathematical calculations.

To obtain the local Rayleigh and Nusselt dimensionless numbers, the physical properties of the fluid are calculated at film temperature:

$$T_f = \frac{T_b + T_w}{2} \tag{1}$$

$$Ra = \frac{\rho c g \beta (T_w - T_b) L^3}{\lambda \nu} \tag{2}$$

$$Nu = \frac{\alpha L}{\lambda} = \frac{qL}{(T_w - T_b)\lambda} \tag{3}$$

defining the plate characteristic thermal length as [15]

$$L = A/p \tag{4}$$

The relative errors on a derived parameter er_F can be evaluated by the propagation law [16]:

$$er_F = \sqrt{\sum_i \left[\frac{x_i}{F(x_i)} \cdot \frac{\partial F(x_i)}{\partial x_i} \cdot er_{x_i} \right]^2} \tag{5}$$

where F is the parameter depending on the variables x_i, which are measured with a known relative error er_{x_i}, calculated by means of the previously mentioned accuracies.

The highest experimental error on the local Nusselt number, obtained in correspondence with the lowest temperature difference between T_w and T_b, is 18.5%.

V. Discussion of Heat Transfer Results

Before the application of the electric field at $q = 690$ $\mathrm{W \cdot m^{-2}}$ with a mean Rayleigh number $\langle Ra \rangle = 3.5 \times 10^8$, a mean Nusselt number on the plate $\langle Nu \rangle = 14.0$ was measured. The heated surface does not cover the entire top face of the vessel; hence, a weak natural convection can build up from the sides of the plate, as shown in Fig. 6, in which the Nusselt number distribution on the plate is displayed.

The blank region on one side of the plate is the missing domain due to the projection on the plate of the central rod, visible in every acquired image of the liquid crystal sheet. In microgravity, the Nusselt number would tend to the unity as the heat transfer process becomes solely of a diffusive nature without any residual buoyant flow.

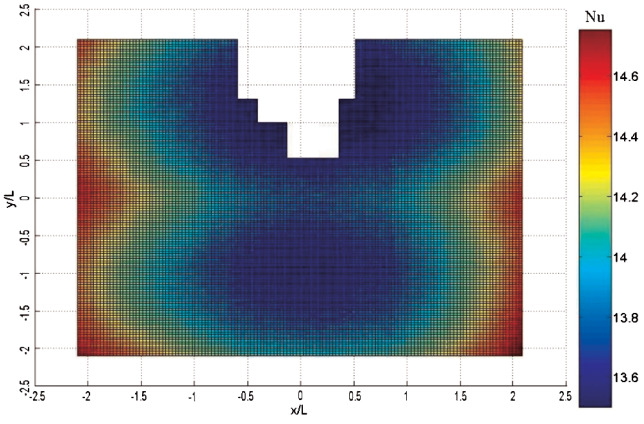

Fig. 6 Nusselt number distribution on the plate at $HV = 0$ and $q = 690$ $\mathrm{W \cdot m^{-2}}$.

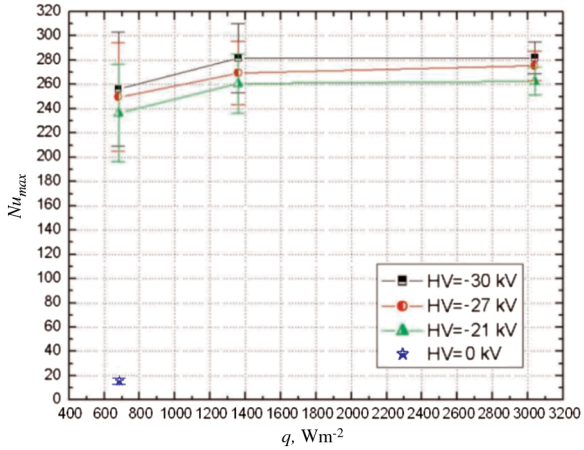

Fig. 7 Nu_{max} vs q at different HV values.

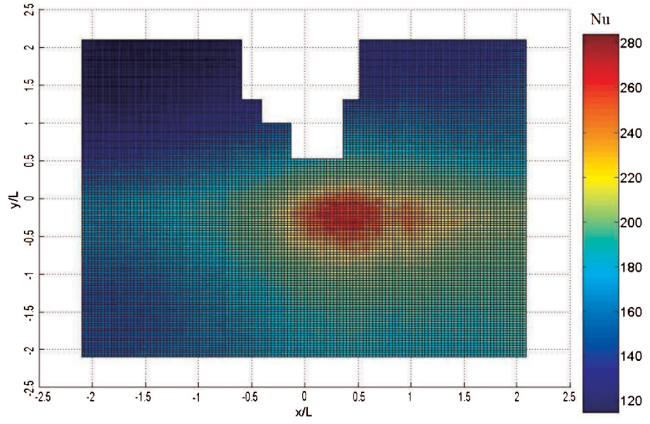

Fig. 8 Nusselt number distribution on the plate at $HV = -30$ kV and $q = 690\ \mathrm{W \cdot m^{-2}}$.

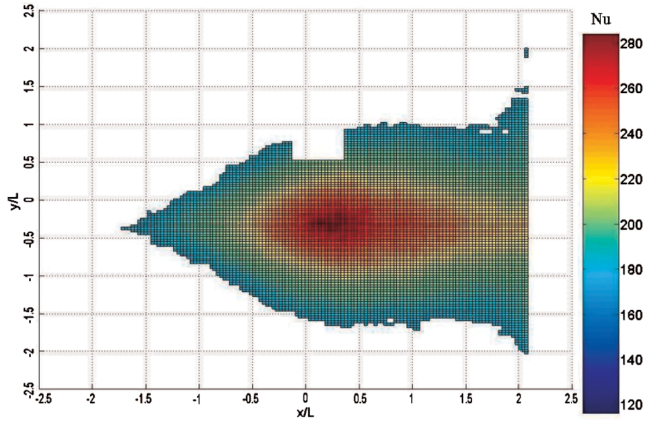

Fig. 9 Nusselt number distribution on the plate at $HV = -30$ kV and $q = 1380\ \mathrm{W \cdot m^{-2}}$.

At the application of the electric field, heat transfer is dramatically augmented. At the three examined high-voltage values, the maximum Nusselt numbers obtained on the plate are plotted in Fig. 7 as a function of the imposed heat flux.

For $HV = -30$ kV and $q = 690\ \mathrm{W \cdot m^{-2}}$, the heat transfer coefficient is increased by over 15 times. In addition, the phenomenon does not seem to be much influenced by thermogravitational effects. In fact, while increasing the heat flux and thus the temperature differences in the fluid, the variations of the maximum Nusselt number remain within the experimental error bands.

Observing Fig. 7, another important practical conclusion can be drawn: is preferable to operate at $HV = -21$ kV, rather than at

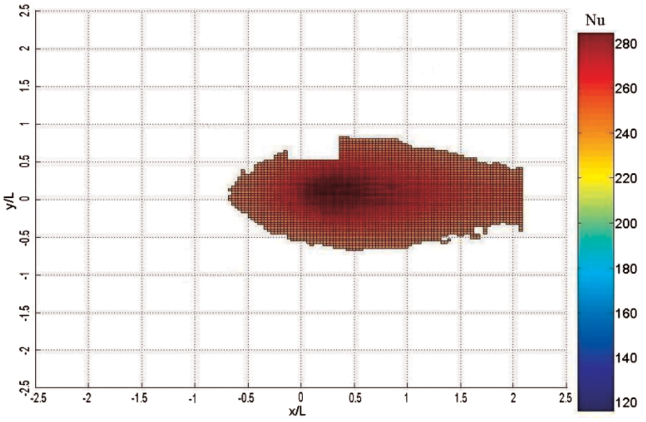

Fig. 10 Nusselt number distribution on the plate at $HV = -30$ kV and $q = 1380\ \mathrm{W \cdot m^{-2}}$.

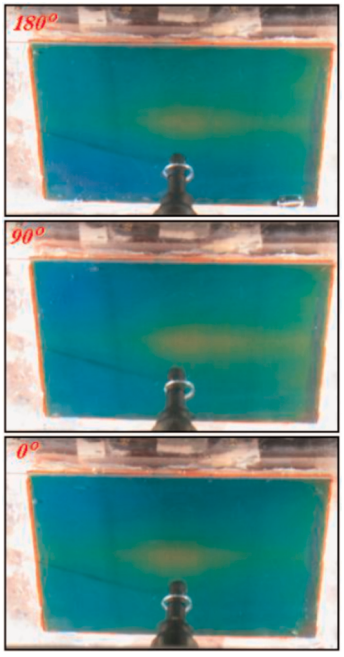

Fig. 11 Effect of the rotation of the point around its axis (0, 90, and 180 deg) on the temperature distribution on the plate.

$HV = -30$ kV, because the enhanced heat transfer rates are only slightly penalized, whereas electrical breakdown is more safely prevented.

Because the highest current measured has been 1.50×10^{-6} A under a negative 30 kV voltage, the maximum power dissipated by the Joule effect is 0.045 W, which is negligible with respect to the introduced heating power of at least 8.5 W; hence, the heat transfer augmentation can be obtained without significant power input.

The Nusselt number contours on the plate, measured in the areas in which the wall temperatures remain within the color-play interval of the TLCs, are illustrated in Figs. 8–10 for the three tested heat-flux values and at $HV = -30$ kV. These distributions are clearly asymmetrical, with one side of the plate sensibly exchanging heat better than the other one. This behavior is typical of inclined submerged jets, for which higher Nusselt numbers on the side of the inclination are expected [17]. The maximum value of the Nusselt number, corresponding to the stagnation point of the EHD-induced jet, is located at a distance of about 1 cm from the axis of the pin.

Rotating the point around its axis, it has been possible to observe the asymmetrical temperature distribution rotate accordingly, as shown in Fig. 11.

The reason for the EHD-induced jet inclination must be searched for in the point superficial microstructure, with nonuniform

microasperities capable of locally enhancing the electric field and thus favoring an inhomogeneous formation of ions.

Long-term tests (over 300 h of continuous operation) have been carried out at $HV = -30$ kV and $q = 690\ \mathrm{W \cdot m^{-2}}$. The liquid has never undergone any electrical breakdown and the heat transfer coefficients, as well as the current, are stable and repeatable after an initial "aging" period, during which an even higher efficiency of the process has been measured.

VI. Conclusions

Very high heat transfer coefficients, enhanced up to 1800%, are obtained on a downward-facing heated plate by means of ion injection, an active technique needing a negligible power input. Heat fluxes typically generated by electronic components have been imposed and it has been shown that the heat exchange phenomenon is dominated by the electrically induced flow, whereas the buoyant forces play only a minor role. An asymmetrical distribution of the Nusselt number, typical of inclined submerged jets, has been observed.

Keeping in mind the analogy between ion injection and submerged impinging jets, interference among different emitters, treated as an array of jets, should be a promising solution for leveling the temperature field on the plate. The performance of the process can then be optimized by working on the number, position, and orientation of the emitting electrodes.

As a further step toward the implementation of the described electrohydrodynamic technique in the design of heat sinks and heat exchangers for the space industry, microgravity research (parabolic flight campaigns) is already planned for assessing the actual heat transfer rates obtainable by ion injection in the complete absence of thermogravitational effects.

Acknowledgments

The author is thoroughly indebted to Walter Grassi for his essential and continuous guidance throughout the research activity and would also like to thank Roberto Manetti for his skilful technical assistance and both Davide Della Vista and Gabriele Torelli for having contributed with great commitment to setting up and running the experimental apparatus. In particular, Gabriele Torelli documented his assistance in the present research activity in [18].

References

[1] Grassi, W., and Testi, D., "Heat Transfer Enhancement by Electric Fields in Several Heat Exchange Regimes," *Annals of the New York Academy of Sciences*, Vol. 1077, Sept. 2006, pp. 527–569.

[2] Ohadi, M. M., Darabi, J., and Roget, B., "Electrode Design, Fabrication, and Materials Science for EHD-Enhanced Heat and Mass Transport," *Annual Review of Heat Transfer*, Begell House, New York, Vol. 11, 2001, pp. 563–632.

[3] Yabe, A., Mori, Y., and Hijikata, K., "Active Heat Transfer Enhancement by Utilizing Electric Fields," *Annual Review of Heat Transfer*, Begell House Inc., New York, Vol. 7, 1996, pp. 1–55.

[4] Grassi, W., Testi, D., and Saputelli, M., "EHD Enhanced Heat Transfer in a Vertical Annulus," *International Communications in Heat and Mass Transfer*, Vol. 32, No. 6, 2005, pp. 748–757.

[5] Grassi, W., and Testi, D., "Heat Transfer Augmentation by Ion Injection in an Annular Duct," *Journal of Heat Transfer*, Vol. 128, No. 3, 2006, pp. 283–289.

[6] Grassi, W., Testi, D., and Saputelli, M., "Heat Transfer Enhancement in a Vertical Annulus by Electrophoretic Forces Acting on a Dielectric Liquid," *International Journal of Thermal Sciences*, Vol. 44, No. 11, 2005, pp. 1072–1077.

[7] Grassi, W., Testi, D., and Della Vista, D., "Heat Transfer Enhancement on the Upper Surface of a Horizontal Heated Plate in a Pool by Ion Injection from a Metallic Point," *Journal of Electrostatics*, Vol. 64, Nos. 7–9, 2006, pp. 574–580.

[8] Felici, N., Gosse, B., and Gosse, J.-P., "La Conduction dans les Liquides Diélectriques: Idées Modernes et Progrès Récents: Aspects Électrochimiques et Électrohydrodynamiques," *Revue Générale de l'électricité*, Vol. 85, No. 11, 1976, pp. 861–874 (in French).

[9] Atten, P., Malraison, B., and Zahn, M., "Electrohydrodynamic Plumes in Point-Plane Geometry," *IEEE Transactions on Dielectrics and Electrical Insulation*, Vol. 4, No. 6, 1997, pp. 710–718.

[10] Felici, N., "High-Field Conduction in Dielectric Liquids Revisited," *IEEE Transactions on Electrical Insulation*, Vol. EI-20, No. 2, 1985, pp. 233–238.

[11] Stishkov, A. Y. K., and Buyanov, A. V., "Electrodynamical Currents in a Wire-Wire Electrode System," *Proceedings of the 14th International Conference on Dielectric Liquids*, Inst. of Electrical and Electronics Engineers, Los Alamitos, CA, pp. 63–66.

[12] Grassi, W., Testi, D., and Della Vista, D., "Optimal Working Fluid and Electrode Configuration for EHD-Enhanced Single-Phase Heat Transfer," Proceedings of the 13th International Heat Transfer Conference (IHTC-13), Assembly for International Heat Transfer Conferences Paper HTE-05, 2006.

[13] Grassi, W., Testi, D., Della Vista, D., and Torelli, G., "Calibration of a Sheet of Thermosensitive Liquid Crystals Viewed Non-Orthogonally," Proceedings of the 60th ATI National Congress, Associazione Termotecnica Italiana Paper 11/03, 2005.

[14] Grassi, W., Testi, D., Della Vista, D., and Torelli, G., "Augmentation of Heat Transfer on the Downward Surface of a Heated Plate by Ion Injection," *Annals of the New York Academy of Sciences*, Vol. 1077, Sept. 2006, pp. 602–612.

[15] Incropera, F. P., and De Witt, D. P., *Fundamentals of Heat and Mass Transfer*, Wiley, New York, 1996, p. 498.

[16] Kline, S. J., and McClintock, F. A., "Describing Uncertainties in Single-Sample Experiments," *Mechanical Engineering*, Vol. 75, 1953, pp. 3–8.

[17] Webb, B. W., and Ma, C.-F., "Single-Phase Liquid Jet Impingement Heat Transfer," *Advances in Heat Transfer*, Vol. 26, 1995, pp. 105–217.

[18] Torelli, G., "Utilizzo dei Cristalli Liquidi Nello Studio Dello Scambio Termico con Ion Injection," B.S. Thesis, Aerospace Engineering, Univ. of Pisa, Pisa, Italy, 2005 (in Italian).